

IMECE2005-82313

HIGH PERFORMANCE HEAT STORAGE AND DISSIPATION TECHNOLOGY

Chanwoo Park

Advanced Cooling Technologies, Inc.,
1046 New Holland Avenue, Lancaster, PA 17601
e-mail: chanwoo.park@1-act.com

Kwang J. Kim

Active Materials and Processing Laboratory
Mechanical Engineering, University of Nevada, Reno, NV 89557

Joseph Gottschlich and Quinn Leland

Air Force Research Laboratory, WPAFB, Dayton, OH

KEYWORDS

Heat storage, metal hydride, phase change material, solid state laser, cooling, heat pipe, directed energy weapon

ABSTRACT

High power solid state laser systems operating in a pulse mode dissipate the transient and excessively large waste heat from the laser diode arrays and gain material. The heat storage option using Phase Change Materials (PCMs) has been considered to manage such peak heat loads not relying on oversized systems for real-time cooling. However, the PCM heat storage systems suffer from the low heat storage densities and poor thermal conductivities of the conventional PCMs, consequently requiring large PCM volumes housed in thermal conductors such as aluminum or graphite foams.

We developed a high performance metal hydride heat storage system for efficient and passive acquisition, storage, transport and dissipation of the transient, high heat flux heat from the high power solid state laser systems. The greater volumetric heat storage capacity of metal hydrides than the conventional PCMs can be translated into very compact systems with shorter heat transfer paths and therefore less thermal resistance. Other exclusive properties of the metal hydride materials consist of fast thermal response and active cooling capability required for the precision temperature control and transient high heat flux cooling.

This paper discusses the operating principle and heat storage performance results of the metal hydride heat storage system through system analysis and prototype testing. The results revealed the superior heat storage performance of the metal hydride system to a

conventional PCM system in terms of temperature excursion and system volume requirement.

NOMENCLATURE

D_p	particle diameter (μm)
E	energy (J)
H/M	hydrogen concentration in metal (or alloy)
H	hydrogen atom
M	metal (alloy) atom
p	pressure (atm)
\dot{Q}	heat flow rate (W)
\bar{R}	universal gas constant ($=8.314\text{kJ/kmole-K}$)
T	temperature (K)
t	time (s)
V	volume (liter)
x	non-stoichiometric constant

Greek

α, β	metal hydride phases
ΔH_f	heat of formation (kJ/H ₂ -kgmole)
ΔS_f	standard entropy of formation (kJ/H ₂ -kgmole-K)

Subscripts

A, B	metal hydride reactors
c	cooling
f	formation or final
h	high
i	initial
l	low
MH	metal hydride
p	particle
r	release
s	heat source or stored

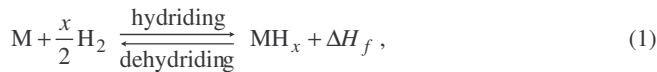
INTRODUCTION

A metal hydride heat storage system integrated with heat pipe was developed for efficient and passive acquisition, storage and dissipation of the transient, high heat flux heat from high power solid state laser systems [Park, 2005]. The multi-kilowatt solid state laser gain material could dissipate the high heat flux waste heat of more than 100W/cm² over a large area as large as 100cm² during the lasing operation. Dissipating such highly-transient heat on real-time basis will require largely oversized cooling systems that might be unaffordable in many applications. Therefore, heat storage systems which store the peak heat and average out the real-time cooling loads greatly help trim the bulky cooling system.

The heat storage systems using conventional PCMs such as paraffin waxes have been considered for temporary heat storage and thermal management [Vrable and Yerkes, 1998; Shanmugasundaram, et. al., 1997; Chow et. al., 1996]. The low heat storage density and poor thermal conductivity of the conventional PCMs make the heat storage option unattractive because of the large PCM volume requirements and necessary heat transfer enhancement using exotic host materials. In contrast, metal hydrides have superior volumetric heat storage capacity to PCMs. For example, Ca_{0.2}M_{0.8}Ni₅, a common hydride, has a heat storage density of 853.3MJ/m³ in raw material condition [Huston and Sandroek, 1980], while paraffin (Calwax 130), a common organic PCM has a heat storage capacity of 177.5MJ/m³ [Al-Hallaj and Selman, 2000]. The greater heat storage density of the metal hydride materials can be directly translated into more compact systems with shorter heat transfer paths making it possible to precisely control the temperature excursion for temperature-sensitive systems.

OPERATING PRINCIPLE

Metal hydrides are the binary combination of hydrogen and a metal or metal alloy. Metal hydrides have been used in many industrial applications such as battery electrode material, hydrogen storage medium and in various thermal systems [Kang et. al., 1996, 1994; Fateev et. al., 1996; Park et. al., 1995; Lloyd et. al., 1998; Kim et. al., 1998a, 1998b, 1998c; Houston and Sanrock, 1980; Shahinpoor and Kim, 2002]. The hydriding (exothermic) and dehydriding (endothermic) reactions of a metal hydride can be expressed as



where M is a metal (or metal alloy), x is a non-stoichiometric constant and ΔH_f is the hydride formation heat. Note that metal hydrides are capable of storing an amount of hydrogen gas (STP) equal to about 1,000 times of their own volume. The hydriding/dehydriding reaction has rapid kinetics and is environmentally clean and safe.

Figures 1(a) and (b) show the Pressure-Hydrogen concentration-Temperature (p -H/M- T) curves for a common metal hydride, LaNi₅H₆ and the van't Hoff plots for variety of commercial hydrides [Houston and Sandroek, 1980] respectively. The p -H/M- T curves and the van't Hoff plots contain the key thermodynamic information required for designing any metal hydride devices and systems.

As shown in Figure 1(a), the hydrogen dissolves within the solid lattice of the metal alloy to form condensed hydride phases following the absorption isotherm curve. All interstitial hydrogen is chemically bonded in the solid lattice. The endpoints, H/M_α and H/M_β, are called

the phase limits of the *plateau* region. An isotherm gives the absolute equilibrium pressure as a function of the hydrogen concentration in alloy, H/M (H=hydrogen atom and M=metal atom). The dehydriding (desorption) isotherm typically lies slightly below the hydriding isotherm due to *hysteresis*. The *hysteresis* is related to an irrecoverable energy loss associated with the volume change of the metal hydride material during the reactions, although the hydriding/dehydriding reactions are generally considered reversible processes.

Figure 1(b) shows the van't Hoff plots of commercially available metal hydrides. Each line describes the equilibrium behavior of a metal hydride at the *mid-point* of the *desorption* isotherm plateau and the equilibrium behavior is expressed as follows:

$$\ln p_{H_2}(\text{atm}) = \frac{\Delta H_f}{RT} - \frac{\Delta S_f}{R}, \quad (2)$$

where \bar{R} is the universal gas constant (8.314kJ/kgmole-K), T is the temperature (K), ΔH_f is the heat of formation (kJ/H₂-kgmole) and ΔS_f is the standard entropy of formation (kJ/H₂-kgmole-K). In the figure, within the temperature range of interest (10~50°C) for the solid state laser cooling, there are various hydrides available from Ca_{0.2}M_{0.8}Ni₅ at higher pressures to Fe_{0.8}Ni_{0.2}Ti at lower pressures.

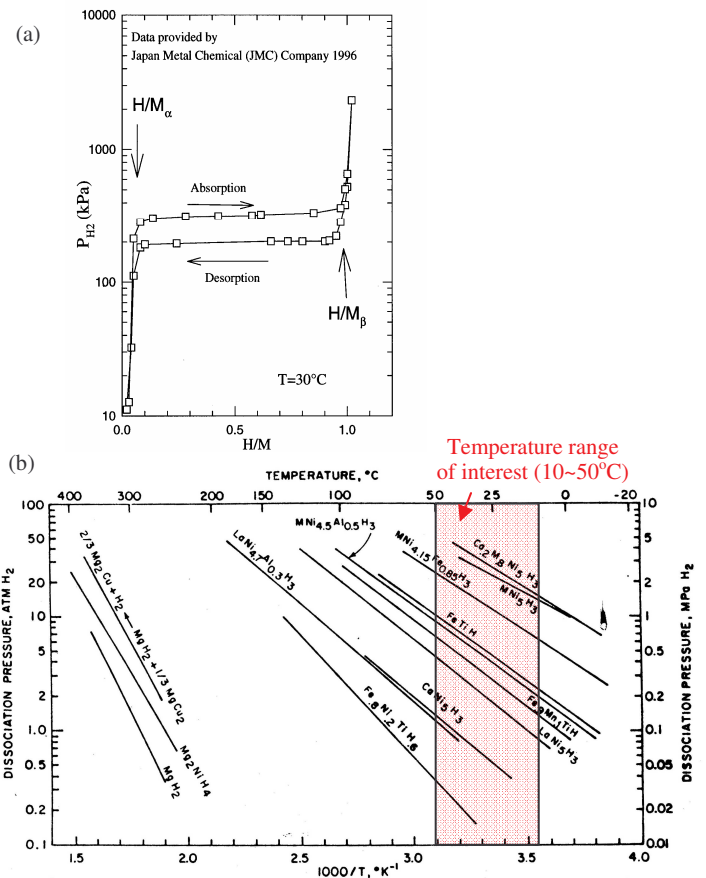


Figure 1 (a) Pressure-H/M-Temperature curves of LaNi₅H₆. (b) van't Hoff plots for various commercial hydrides [Houston and Sandroek, 1980].

The proposed metal hydride heat storage and dissipation system (patent pending) is illustrated in Figure 2. It consists of a heat pipe (or vapor chamber) and a metal hydride bed. The modular design is readily scalable to larger-area heat sources by simply multiplying the

module. In the solid state laser system, the laser gain material in slab shape may dissipate the waste heat more than $100\text{W}/\text{cm}^2$ over an area as large as 100cm^2 (i.e., total thermal energy of 10kW) during a 5-minute lasing. During the laser operation, the laser slab temperature should be maintained within the maximum spatial and temporal variations to avoid the harmful thermal stresses leading mechanical fracture and to enhance the optical output respectively. Typical laser operating cycle for Directed Energy Weapon (DEW) applications consists of two operating modes: an active period (lasing or standby) such as 5 minutes and a much longer “regeneration” period such as 90 minutes which depends on the heat rejection capability. The metal hydride system can temporarily store the excessive laser heat load during the short heat storage operation and later dissipate the cooling loads distributed over the extended regeneration period using a downsized cooling system.

Figure 2(a) shows the “heat storage” operation of the metal hydride system. The heat pipe acquires the heat load (Q) from a heat source and transports most of the heat load (Q_s) to the metal hydride bed where the dehydriding (endothermic) reaction takes place. The released hydrogen gas during the dehydriding reaction is temporarily stored in a remote container for the hydrogen recovery during the next duty cycle. The remaining heat (Q_c) except for the stored heat (Q_s) is continuously rejected from a portion of the heat pipe condenser section to an ultimate heat sink using a heat rejection system through either radiation or convection, depending on the application.

During the subsequent “regeneration” period as shown in Figure 2(b), when the heat loading stops, the entire module has to be cooled down to recover the initial temperature conditions. The cooling forces the metal hydride to re-absorb the released hydrogen gas through the hydriding (exothermic) reaction. The regeneration completes a full cycle. The system is now ready for the next duty cycle.

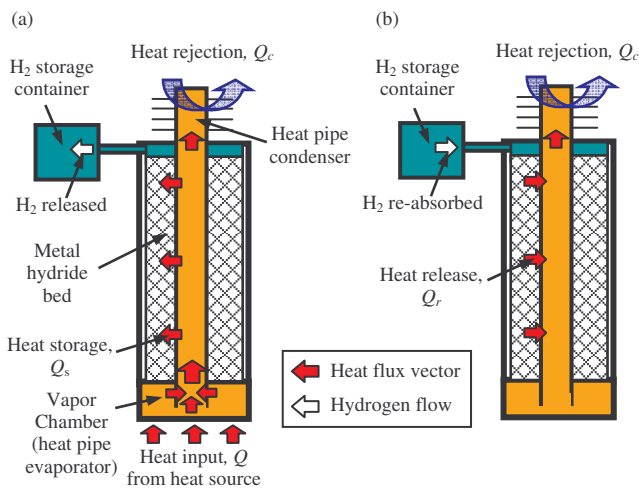


Figure 2 Operating principle of proposed metal hydride heat storage system: (a) heat storage and (b) regeneration operations.

In Figure 3, the proposed heat storage concept was re-explained using the pressure-H/M-temperature curves. During the “heat storage” period, the metal hydride absorbs the heat from a heat source and releases hydrogen in the dehydriding process starting from the initial state (point A) to the final state (point B). During the subsequent “regeneration” period, the metal hydride is cooled down by the heat

rejection system and absorbs the released hydrogen following from point B to point A. The operation is a fully temperature-driven and nearly reversible process. ΔT_{MH} and Δp_{H_2} are the temperature and pressure excursions during a heat storage cycle, respectively.

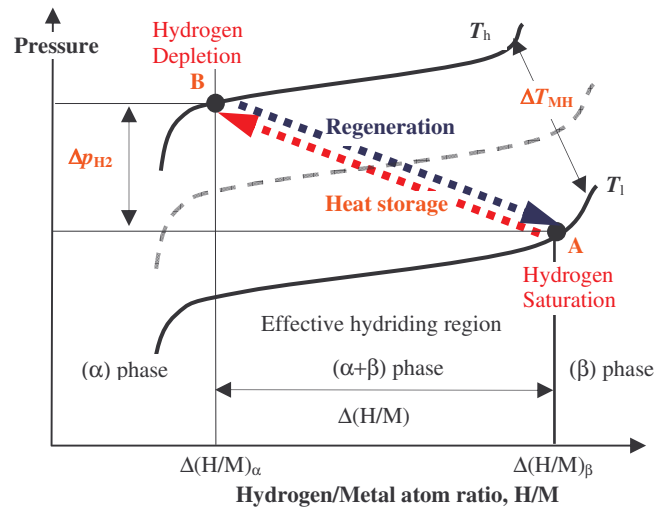


Figure 3 Pressure-H/M-Temperature curves explaining proposed concept.

The proposed metal hydride system adapted the “micro-encapsulation” technique to enhance the thermal conductivity of the metal hydrides. This technique coats the hydride powders with a thin copper layer and compresses the coated powders into porous pellets. Figure 4 shows the SEM (Scanning Electron Microscope) photograph of LaNi_5 particles ($D_p \sim 40\mu\text{m}$) encapsulated by a thin copper layer (thickness $\sim 1\mu\text{m}$) and an annular metal hydride pellet using the copper-coated metal hydrides. Briefing speaking of the micro encapsulation process, first of all, the metal hydrides are sieved to a diameter D_p of $25\sim 40\mu\text{m}$ and then micro-encapsulated with a thin copper skin (which is permeable to hydrogen gas) using an electroless plating technique. Then, the micro-encapsulated particles are mixed with a small amount of metallic binders and pressed into metal hydride pellets. Previous experiments measured the thermal conductivity of these pellets at 5 to $7\text{W}/\text{m}\cdot\text{K}$, more than 50 times of untreated powder beds ($\sim 0.1\text{W}/\text{m}\cdot\text{K}$) [Lloyd et al., 1998].

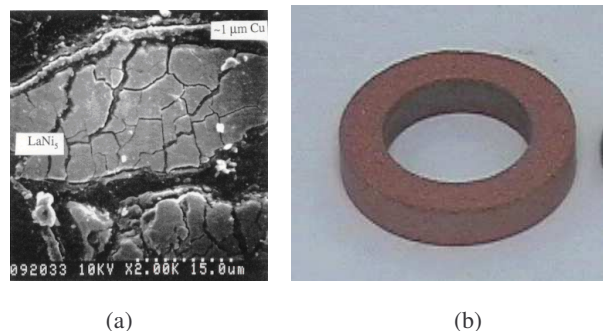


Figure 4(a) SEM photograph of micro-encapsulated LaNi_5 (decrepitation of LaNi_5 is clearly shown) [Kim et al., 1998a]. (b) A photograph of a metal hydride pellet (center hole is for heat pipe insertion) [Park, 2005].

SYSTEM STUDY AND DISCUSSION

One of the design considerations for the efficient metal hydride heat storage system is how to create and sustain favorable hydrogen pressure boundary conditions during the dehydriding (endothermic) reaction. The hydrogen gas released during the heat storage period needs to be removed out of the heat storage system into a relatively large container to sustain the active dehydriding process. Otherwise, excessively built-up hydrogen pressure in the system retards the dehydriding reaction consuming the heat (i.e., endothermic reaction) and eventually raises the metal hydride temperature resulting in degrading heat acquisition. Note that, since the hydrogen storage container can be remotely located away from the main heat storage system as shown in Figure 2, the metal hydride system can be designed in a very compact form factor. The system study using four different hydrogen storage options was briefly discussed as follows:

Option 1: Hydrogen container: As shown in Figure 2, during the heat storage period, the released hydrogen gas is stored in a hydrogen storage container. During the subsequent regeneration, the hydrogen is recovered from the hydrogen container. Although this option is most simple and reliable, the hydrogen container volume may be relatively large as compared to the metal hydride volume. The thermal energy E_s stored in a metal hydride is determined by the amount of released hydrogen gas n_{H_2} (H_2 -kgmole). Since the hydrogen container pressure can be approximated to the metal hydride pressure, assuming that the hydrogen gas is stored in a container (V_{H_2}) at the ambient temperature T_∞ , the stored thermal energy E_s can be estimated as

$$E_s = \Delta H_f n_{H_2} = \Delta H_f \left(\frac{\Delta p_{H_2} V_{H_2}}{RT_\infty} \right), \quad (3)$$

where, using Eq. (2),

$$\Delta p_{H_2} = \exp \left[\frac{\Delta H_f}{RT_{MH,f}} - \frac{\Delta S_f}{R} \right] - \exp \left[\frac{\Delta H_f}{RT_{MH,i}} - \frac{\Delta S_f}{R} \right]. \quad (4)$$

Here $T_{MH,i}$ and $T_{MH,f}$ are the initial and final temperatures of the metal hydride during the heat storage mode respectively. Δp_{H_2} is the pressure change in the hydrogen storage container (atm). From Eq. (3) showing that E_s is linearly proportional to the Δp_{H_2} and the hydrogen container volume V_{H_2} , it is concluded that more heat storage for a given hydrogen container volume is realized by a larger hydrogen pressure rise Δp_{H_2} .

Option 2: Hydrogen vent/recharging: During the heat storage period, the released hydrogen gas is vented to the ambient or fed to other systems that would consume the hydrogen gas (e.g. fuel cells). During the following regeneration, fresh hydrogen from high-pressure hydrogen tanks (e.g., 10,000psi) is recharged to the metal hydride system. The hydrogen recharge capacity limits the number of duty cycle.

Option 3: Mechanical compression: During the heat storage period, the released hydrogen gas is stored in a hydrogen container. During the next regeneration, a mechanical compressor is used to return the hydrogen back to the metal hydride. This option requires an electrical power source to operate the compressor. While the compressor can assist the hydrogen storage during the heat storage operation, the vibration from the compressor during the lasing can be avoided if it is used only for the regeneration. The volume requirement would be less than the option 1.

Option 4: Thermal compression using dual metal hydrides:

During the heat storage period, the released hydrogen gas is stored in a remotely-located secondary metal hydride container having a different kind of metal hydride than the main metal hydride which stores the heat from the heat source. During the subsequent regeneration, the temperature of the secondary hydride is elevated by external heating means to increase the hydrogen pressure and drive the hydrogen back to the primary metal hydride. This option requires a thermal energy source (e.g., electrical heater or waste heat). However, the thermal compression doesn't involve any mechanical moving parts unlike mechanical compressors. The volume requirement will be the least among the options or equal to the option 3.

The option 4 is discussed in detail at the following paragraphs. Figure 5 illustrates the operating principle of the option 4 using the dual metal hydride system of MH_A and MH_B . The figure shows the heat fluxes and hydrogen flows between the two hydride reactors. During the "heat storage" period, a heat load Q_A being stored into MH_A initiates the dehydriding (endothermic) reaction that releases the hydrogen gas. At the same time, as a valve in the hydrogen transport line opens, the hydrogen released from MH_A is freely transferred to MH_B due to the pressure differential between the hydride reactors. Consequently, the hydriding (exothermic) reaction in MH_B generates the internal heat (Q_B) which increases the temperature or pressure of MH_B until the pressure equilibrium is reached in the system.

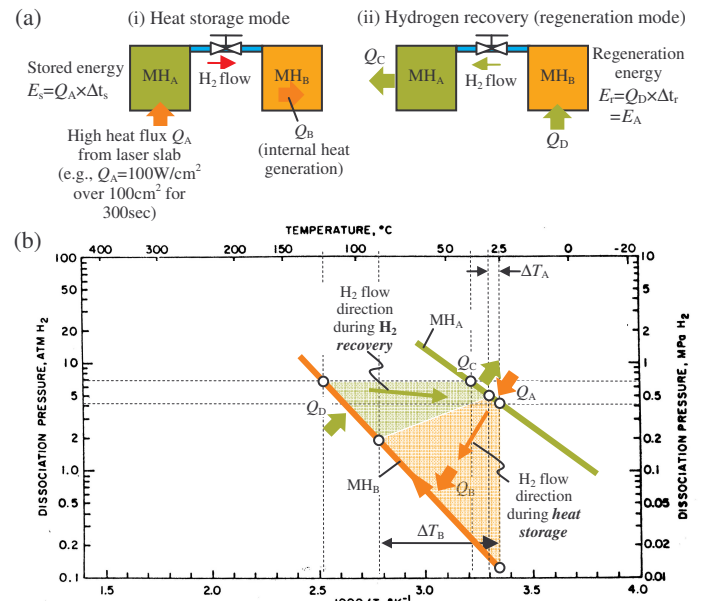


Figure 5(a) Principle of operation using "dual hydrides" of MH_A and MH_B and (b) van't Hoff diagram explaining the heat storage and regeneration operation.

The subsequent regeneration operation consists of two modes: "hydrogen recovery" and "system cooling". During the hydrogen recovery following the heat storage, an external heat Q_D is applied to MH_B in order to raise the hydrogen pressure of MH_B (i.e., thermal compression) and therefore to reverse the hydrogen flow. Once all the hydrogen is fully recovered by MH_A , the valve in the hydrogen transport line is shut off to prevent the hydrogen from reversing. During the subsequent "system cooling" period (not shown in Figure 5), both metal hydride reactors are cooled down to the initial

temperatures to be ready for the next duty cycle. The thermal energy E_r required for the regeneration equals the stored energy E_s . Therefore, the total heat rejection to ambient for a completed cycle is doubled.

Q_D required for the regeneration can be much smaller than Q_A from the heat source if a longer regeneration period is allowed. As a result, the spontaneous coefficient of performance ($COP_C = Q_A/Q_D$) of the dual hydride system can be much greater than unity. Note that Q_A and Q_D are the heat transfer rates (Wattage), not total heat transferred (Joule). Also note that a common air-cooled vapor compression system has a COP_C of about 3.

A comparison study was conducted among competing technologies including PCM, metal hydrides and ammonia. The system study was performed for an 1MJ heat storage and the results are summarized in Table 1. The system study assumed that beside the host structure (i.e., heat pipe and container), paraffin wax (Calwax 130) is contained in an aluminum (Al) foam of 20vol.% and the metal hydride was mixed with Copper (Cu) and Tin (Sn) of 17vol.% for thermal conductivity enhancement. Based on the prototype design which will be discussed in the next section, the volume ratio of the host structure to the heat storage materials was assumed to be 1.0. The core heat storage volume (V_1) includes the heat storage material and host structural volumes. Note that hydride and ammonia systems require additional gas storage volumes (V_2) unlike the PCM system.

Table 1 Comparison of various latent heat storage technologies.

	Paraffin (Calwax 130)	Single MH (Ca-based)	Dual MH (Ca/Fe-based)	Ammonia [^] (NH ₃)
Raw material volume (l/MJ)	6.2	1.0	4.6	1.4
Effective latent heat ⁺ , ΔH (MJ/m ³)	78.1	351.8	351.8	702.7
Core heat storage volume (l/MJ), $V_1 = Q/\Delta H$	12.8*	2.8*	2.8*	1.4
Gas storage volume, V_2 (l/MJ)	0	26.4	8.2	109.9
System volume, $V_3 = V_1 + V_2$ (l/MJ)	12.8	29.2	11.1	109.9
Max. system pressure (atm)	~1	39.5	16.6	9.9
Idling system pressure (atm)	~1	13.1	4.1	9.9
Temperature excursion [†] (°C)	>60°C	>20°C	±3°C	>5°C

+ The latent heat was calculated including the heat transfer host structure and thermal conductivity enhancement materials.

* Based on a prototype design, the heat pipe/heat storage material volume ratio was assumed to be 1.0.

[^] Based at the ammonia saturation temperature of $T=25^\circ\text{C}$.

[†] Based on the preliminary system study performed for this work.

For the single metal hydride (MH) system, the core heat storage volume (V_1) is estimated to be 2.8 liters and by adding the additional hydrogen storage volume (V_2) of 26.4 liters, the total system volume (V_3) becomes 29.2 liters. In contrast, for the paraffin wax system, the

total system volume (V_3) is estimated to be 12.8 liters. Note that the core heat storage volume (V_1) of the metal hydride systems is 4.5 times smaller than the PCM system because of the greater heat storage density of the metal hydride materials. The hydrogen storage volume (V_2) for the metal hydride systems is only for storing the hydrogen and does not directly participate in the heat storage process.

Because of the great hydrogen storage density of the metal hydride materials, the secondary hydride in the dual hydride system can store the hydrogen in a dramatically reduced volume (V_2) as compared to the single metal hydride system. As a result, the dual hydride system volume (V_3) is about 13.5% smaller than the paraffin wax system. An ammonia system was estimated by assuming all heat input is used to vaporize liquid-phase ammonia at 25°C to vapor-phase ammonia at 50°C . The estimation didn't include any required active liquid pumping or the condenser which would be required for the ammonia system.

PROTOTYPE TESTING AND RESULTS

In order to demonstrate the metal hydride heat storage technology, a small-scale prototype system was designed, built and tested. Figure 6 shows the test setup that consists of a metal hydride heat storage module and a hydrogen handling system. The metal hydride container volume is 99cc. Four hydrogen containers of 123cc, 2, 4 and 8 liter were used for examining the effect of the hydrogen container volume on the heat storage performance. Combination of the four hydrogen containers provides various volumes from 123cc up to 14.1 liters.

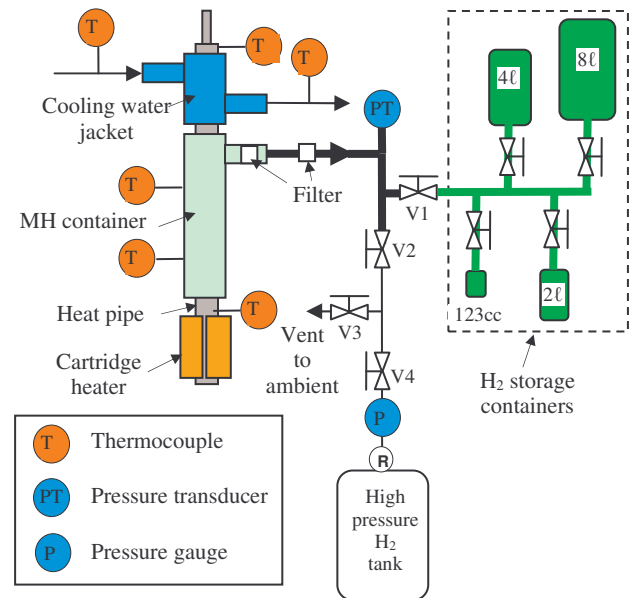


Figure 6 Test setup for prototype metal hydride heat storage system.

For the direct comparison, an identical heat storage system was also built using a paraffin wax (manufacturer: Rubitherm GmbH, model No. Rubitherm RT 35, melting temperature: 35°C) and tested alongside. Electrical cartridge heaters were used as a heat source and a cooling water jacket was used for cooling the heat storage module. Two thermocouples probed in the heat storage material container were used to measure the temperatures of each heat storage material. For the

metal hydride system, a pressure transducer (manufacturer: Omega, model No. PX303, $p_{max}=1,000\text{psig}$) was used to monitor the transient pressure variation during the testing.

Figure 7(a) shows the measured temperature and pressure profiles at the baseline condition: 200W heat input for 300 seconds and a fixed hydrogen gas storage volume of 10 liters under the pressure equilibrium with the metal hydride reactor. As shown in Figure 7(a), once the heat load of 200W was applied, the heat source temperatures rapidly increased and are followed by the heat storage material temperatures: the metal hydride temperature is much closer to the heat source temperature than the wax. This indicates that the metal hydride system has less heat source-to-sink thermal resistance. At the end of the heating period (300 seconds), the heat source temperature of the metal hydride system reached 47.7°C , while the heat source temperature in the PCM system reached 62.8°C . Note that the peak wax temperature was well above the melting temperature (35°C), indicating that all the wax had melted.

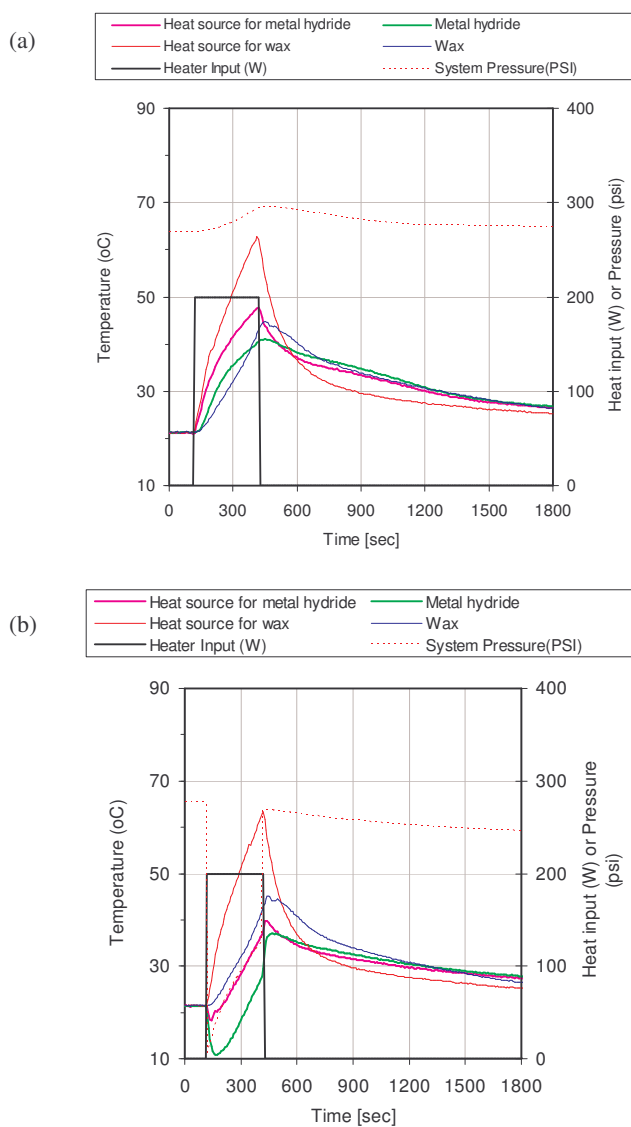


Figure 7 Measured temperature and pressure profiles at the baseline condition with (a) a 10 liter hydrogen container volume and (b) with a 4 liter hydrogen container volume.

Figure 7(b) shows the temperature results at the same conditions except the hydrogen conditions: the hydrogen container volume was reduced to 4 liters under initial vacuum. The vacuum container was used to simulate the initially low pressure conditions likely found in Options 2, 3 and 4. The test results clearly show that the metal hydride system is very capable of storing the heat of 60kJ ($=200\text{W} \times 300\text{s}$) with the temperature excursion under the maximum allowance of 25°C . With a 200W heat input for 300 seconds, the heat source temperature rise of the metal hydride system was 16.1°C , while the PCM had a 41.6°C in the temperature rise.

As shown in Figures 8(a)-(c), parametric testing was performed using various hydrogen storage volumes, heat storage periods and hydrogen initial charges against heat inputs, respectively. Figure 8(a) shows the effect of the hydrogen storage volume on the heat source temperature rise. First, with a hydrogen container volume of 123cc (the smallest), the heat source temperature excursion is still smaller than the wax system. Larger hydrogen container volumes resulted in even lower temperature excursions. For a heat input of 312.5W with a hydrogen container volume of 4 liter under vacuum, the metal hydride system had a temperature rise of 30.6°C , which is 31.4°C lower than the temperature excursion of 62.0°C in the wax system under the same condition.

Figure 8(b) shows the effect of the heating period on the temperature excursion. For the extended heating period of 600 seconds, the temperature excursion of the wax system increases exponentially unlike the case of the heating period of 300 seconds. This indicates that at 200W heat load for 600seconds, the wax system has stored the heat in the form of sensible heat which speeds up the temperature rise. Figure 8(c) shows the effect of the initial hydrogen charge in the metal hydride system for the temperature excursion. Before each testing, the fresh hydrogen was charged to the metal hydride heat storage container. Although the smaller initial hydrogen charge gave a better performance, further decrease in the hydrogen charge will increase the temperature excursion because of the lack of the hydrogen. Therefore, an optimum for initial hydrogen charge would exist at a low range.

CONCLUSIONS

Based upon the system study and prototype testing, the following conclusions can be made.

- **Precision temperature control:** The prototype metal hydride device successfully demonstrated an excellent temperature control performance. The metal hydride device was able to control the temperature excursion within 30.6°C at a 313W heat input for 300 seconds. An identically sized PCM device exhibited a temperature excursion of 62°C . The heat input of 313W corresponds to a heat flux of $61.8\text{W}/\text{cm}^2$ based on the heat source area.
- **Greater heat storage capacity:** For an 1MJ heat storage, the total volume of a dual metal hydride design was estimated to be 11.1 liter. This volume is 13.5% smaller than a typical PCM system. Noticeably, the heat storage volume of the metal hydride unit was much smaller than the PCM system (less than 25%).
- **Robust and reliable operation:** Since the metal hydride system can be thermally driven with no mechanical moving parts, the operation is robust and reliable.

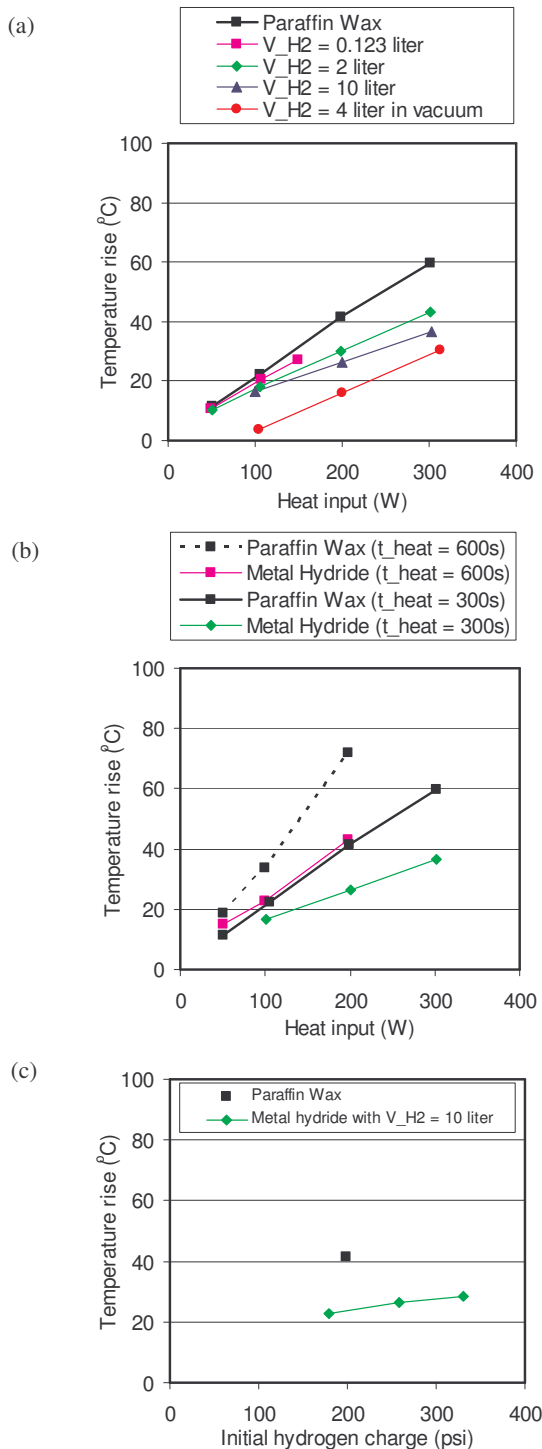


Figure 8 Effect of (a) heat input, (b) heating period and (c) initial hydrogen charge on heat source temperature excursion.

ACKNOWLEDGMENT

This work was performed under MDA STTR Phase I Contract No. FA8650-04-M-2517. The authors wish to acknowledge the contributions of Mr. David Sarraf and Mr. Jay Weaver, both of Advanced Cooling Technologies, Inc. for their efforts in the drawing and testing of the metal hydride system. Also, KJK acknowledges the

help from his graduate students, D. Kim and S. Vemuri, regarding micro-encapsulation of metal hydrides.

REFERENCES

1. Chanwoo Park, 2005, "Passive High Performance Heat Storage and Dissipation Technology for Transient High Power Thermal Management," MDA STTR Phase I Final Report FA8650-04-M-2517.
2. D.L. Vrable and K.L. Yerkes, 1998, "A Thermal Management Concept for More Electric Aircraft Power System Application," SAE Transactions, 981289.
3. V. Shanmugasundaram, J.R. Brown and K.L. Yerkes, 1997, "Thermal Management of High Heat-Flux Sources Using Phase Change Materials: A Design Optimization Procedures," American Institute of Aeronautics and Astronautics, Proceedings of the 32nd Thermophysics conference, June 23-25, AIAA-97-2451.
4. L.C. Chow, J.K. Zhang and J.E. Bean, 1996, "Thermal Conductivity Enhancement for Phase Change Storage Media," Int. Comm. Heat Mass Transfer, Vol.23, No.1, pp.91-100.
5. E.L. Huston and G.D. Sandrock, 1980, "Engineering Properties of Metal Hydrides," Journal of Less Common Metals, Vol.74, pp.435-443.
6. S. Al-Hallaj and J.R. Selman, 2000, "A Novel Thermal Management System for Electric Vehicle Batteries using Phase-Change Material," Journal of the Electrochemical Society, Vol.147, No.9, pp.3231-3236.
7. B.H. Kang, C.-W. Park, and C.S. Lee, 1996, "Dynamic Behavior of Heat and Hydrogen Transfer in a Metal Hydride Cooling System," International Journal of Hydrogen Energy, Vol.21, No.9, pp.769-774.
8. G.A. Fateev, B.H. Kang, K.J. Kim and C.-W. Park, 1996. "Numerical Simulation And Experimental Investigation of Heat Conversion Cycle in Metal Hydride Media," Heat/mass Transfer-MIF-96 Heat and Mass Transfer in Capillary-Porous Bodies, A.V. Luikov Heat and Mass Transfer Institute, Minsk, Vol.7, pp.169-182.
9. C.-W. Park, B.H. Kang, S. Jeong and C.S. Lee, 1995, "An Experimental Study of Heat and Mass Transfer during Absorption and Desorption Processes in a Hydride Material Bed," Journal of Korean Society of Mechanical Engineering, Vol.19, No.1, pp.202-211 (in Korean).
10. B.H. Kang, C.-W. Park, and C.S. Lee, 1994, "Dynamic Behavior of Heat And Hydrogen Transfer in a Metal Hydride Chiller," 1994 ICR.
11. G.K. Lloyd, K.J. Kim, K.T. Feldman, Jr., and A. Razani, 1998 "Thermal Conductivity Measurements of Metal Hydride Compacts Developed for High-Power Reactors," AIAA-Journal of Thermophysics and Heat Transfer, Vol.12, No.2, pp.132-137.
12. K.J., Kim, K.T. Feldman, Jr., G.K. Lloyd and A. Razani, 1998a, "Compressor-Driven Heat Pumps Development Employing Porous Metal Hydride Compacts," ASHRAE Transactions, 1998-Winter Meeting, San Francisco, Vol.104, Pt.1, SF-98-18-4.
13. K.J. Kim, G.K. Lloyd, A. Razani, and K.T. Feldman, Jr., 1998b, "Development of LaNi₅/Cu/Sn Metal Hydride Powder Composites," Powder Technology-An International Journal, Vol.99, pp.40-45.
14. K.J. Kim, G. Lloyd, K. T. Feldman, Jr., and A. Razani, 1998c, "Thermal Analysis of the Ca_{40.4}Mm_{0.6}Ni₅ Metal-Hydride Reactor," Applied Thermal Engineering, Vol.18, No.12, pp.1325-1336.
15. K.J. Kim, Personal communication, 1996-2004.
16. M. Shahinpoor and K.J. Kim, 2002, "Novel Metal Hydride Artificial Muscles," U.S. Patent #6,405,532.